

REACTION SPHERE FOR ATTITUDE CONTROL

E. Onillon⁽¹⁾, O. Chételat, L. Rossini, L. Lisowski, S. Droz, J. Moerschell⁽²⁾

⁽¹⁾CSEM, Jacquet Droz 1, 2002 Neuchâtel Switzerland, Email: emmanuel.onillon@csem.ch

⁽²⁾HEVS, Case postale 2134 Route du Rawyl 471950 Sion 2, Email: joseph.moerschell@hevs.ch

ABSTRACT

In the frame of an ESA project, CSEM in collaboration with RUAG has developed an innovative Attitude Orbit Control System concept that relies on a Reaction Sphere. We propose to use one unique reaction sphere playing both the role of ‘reaction sphere’ and (as the angular velocity of the sphere increases) the role of ‘control moment gyro’. Based on analytical models, the expected performances for the selected reaction sphere of 14.1 kg spinning at 6000 rpm are a torque of 6 Nm for 70 W and an angular momentum of 27 Nms. A Reaction Sphere prototype has been manufactured based on an eight pole permanent magnet rotor and a 20 pole stator. Preliminary tests to validate the Reaction Sphere model are currently in progress.

1. INTRODUCTION

An Attitude Control System (ACS) traditionally requires a minimum of three reaction wheels (in practice, four wheels are common because the system can be better optimized and the extra wheel allows for failure recovery). Hence, the orientation of the satellite can be changed by accelerating the appropriate wheel. Another traditional approach is to use a control moment gyro consisting of a rapidly rotating wheel held by gimbals. Applying torques on the gimbals joints changes the satellite orientation.

The proposed approach is to use one unique Reaction Sphere playing both the role of ‘reaction sphere’ and—as the angular velocity of the sphere increases—the role of ‘control moment gyro’. The Reaction Sphere is held in position by magnetic levitation and can be accelerated about any rotation axis by a 3D motor. The torque required for this acceleration is exported to the satellite and is used to change the satellite attitude.

ACSs have long been recognized among the main spacecraft subsystems and there is an interest to reduce their mass and volume. An ACS based on a Reaction Sphere would be smaller and lighter than today commonly employed systems and related costs are expected to be lower as well. Because of its unparalleled symmetry, the CSEM Reaction Sphere does constantly deliver a maximum inertia whatever its current rotation axis. From this point of view, a sphere is the most compact and natural way of making an ACS. The possibility of using the gyroscopic effect for increasing the velocity of the sphere is also an attractive feature

that may significantly reduce the frequency of desaturation.

Although the concept of Reaction Sphere is not new, limitations of existing technologies and engineering capabilities have prevented its development. The challenge is clearly focused on the 3D motor, on the magnetic bearing, and their combination. However, recent advances in simulation and modeling, power electronics, sensing, and especially in high-power Space-qualified processors give a totally new chance to the Reaction Sphere.

Based on the previously developed models, the expected performances for the selected reaction sphere of 14.1 kg spinning at 6000 rpm are a torque of 0.2 Nm and an angular momentum of 23 Nms. Notice that, for a mass equivalent to three reaction wheels, with the Reaction Sphere concept we expect a smaller volume, a higher torque (factor 30) and higher inertia momentum (factor 2).

The present paper describes the Reaction Sphere concept, design and preliminary tests. The presented concept is protected under the patent WO 2007/113666 A2.

2. REACTION SPHERE CONCEPT SELECTION

2.1. Possible motor types

During the concept study phase, several types of possible 3D motors have been considered:

Type 1: Inductive motor (asynchronous motor) with a rotor made of non-conductive ferromagnetic sphere coated with a layer of conductive material (*Figure 1*, top left).

Type 2: Permanent-magnet motor (synchronous motor) with a 8-pole permanent-magnet rotor (*Figure 1*, top right).

Type 3: Reluctant motor (synchronous motor) with a 8-pole ferromagnetic star (*Figure 1*, bottom).

The reluctant motor (type 3) was immediately discarded because of its intrinsic nonlinear nature.

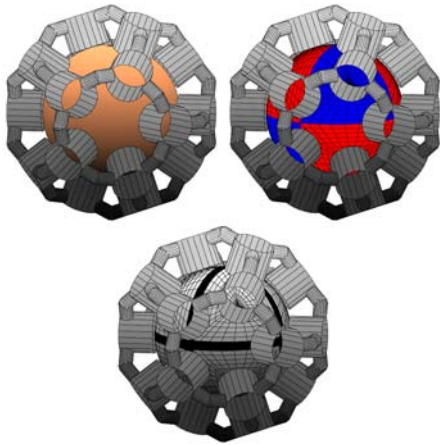


Figure 1: Possible type of motors

2.2. Reaction Sphere Rotor Analysis

Inductive Motor (type 1)

The rotor of the inductive motor is a spherically symmetric sphere made of ferromagnetic material coated with a layer of conductive material (e.g. copper). The core ferromagnetic material is low conductor as to limit the internal eddy currents that would reduce the efficiency. The rotor may be hollow to optimize the inertia-moment-to-mass ratio, but a solid sphere allows the field to go through it straighter making a larger part of the eddy currents to contribute to the torque.

However, the inductive motor concept has been discarded because of its poor efficiency. To illustrate, torque is made as a consequence of eddy currents, which dissipate thermal energy. Even worse, not all eddy currents contribute to the torque, and some may induce vibrations. Finally, this concept presents non-linearities that complexify the controller design of such a system.

Permanent-magnet Motor (type 2)

A 3-D permanent-magnet motor is obtained with a multi pole rotor. In order to keep as much symmetry as possible, the number of regularly distributed poles on a sphere follows the number of vertices of the regular polyhedrons, i.e., 4 (tetrahedron), 6 (hexahedron), 8 (cube), 12 (icosahedron), and 20 (dodecahedron). Of these five polyhedrons, only the cube has faces with an even number of edges and only its vertices can therefore be alternatively the north and south poles of a permanent magnet. As shown in **Figure 2**, a cubic distribution applied to the sphere means a sphere split into height quarters, each of them being either a north pole if $xyz > 0$ or a south pole otherwise (x , y , and z are the coordinates of a given point of the sphere).

Contrary to the inductive concept, the permanent-magnet synchronous motor presents the advantage of its linearity (current to force/torque). As consequence, the bearing and motor functions can be decoupled, easing the design and the development of a pure analytic model of the system. Torque and force productions are also decoupled. All losses associated with the rotor of the induction motor are absent in this design and there is virtually no eddy current induced in the rotor.

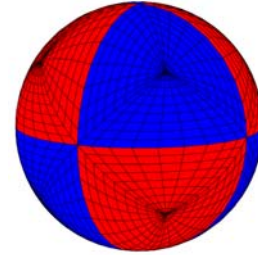


Figure 2: 8-pole permanent-magnet rotor

2.3. Reaction Sphere Stator Analysis

Only bipolar and 8-polar rotating fields are possible. Note, however, that a bipolar rotating field has some singularities: for a vertical magnetic field, a rotation about the vertical axis is not possible without a discontinuity. More generally, to be efficient, the field must be perpendicular to the instantaneous rotation axis. A change of the rotation axis generally does not preserve this property without a discontinuity. Only 2D motors can be used with a bipolar field. For a reaction-gyro sphere, a 2D motor is not acceptable because the rotation around the bipolar axis is uncontrolled. For 3D motors, only the 8-polar rotating field is possible.

A 20-pole stator can produce an 8-polar rotating field in a symmetric manner since five cubes can share the vertices of the dodecahedron. However, observe that a 12-pole stator cannot be used as it resulted to have singular configurations as the one presented in **Figure 3**.

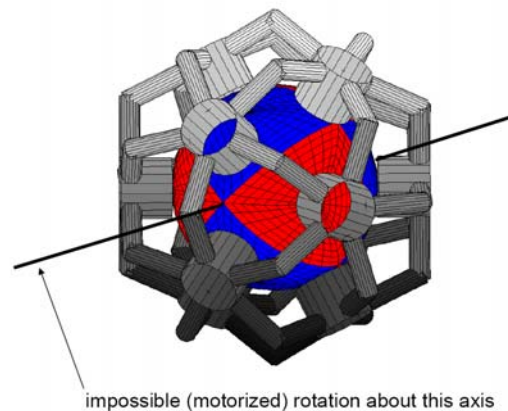


Figure 3: 12-pole stator singularity

Therefore, the 20-pole stator is the only choice to produce such a field. Moreover, a 20-pole stator is good for the bearing of an 8-pole rotor or a spherically symmetric rotor. Finally, the stator has 20 poles, each corresponding to one vertex of the dodecahedron. The coils can be adjusted around the poles (20 coils) or around the bridges linking two adjacent poles (30 coils).

3. REACTION SPHERE MODEL

3.1. Immobile Isolated Rotor

The linearity of the synchronous concept allows the analytical writing of physical parameters (force, torque, inductance and field), in case of a non-shielded and a shielded stator. The magnetic potential outside an isolated eight pole rotor is related to the spherical harmonic Y_3^2 , which is the fundamental for the cubic configuration of the rotor and satisfies the Laplace's equation $\nabla^2\Theta = 0$. The following potential complies with these conditions:

$$\Theta(x, y, z) = \frac{3\sqrt{3}B_0r_2^5}{4\mu_0} \frac{xyz}{r^7} \quad (1)$$

where B_0 is the maximum of the flux density at the surface of the rotor delimited by the radius r_2 , μ_0 is the vacuum permeability, and $r^2 = x^2 + y^2 + z^2$. Assuming the rotor immobile and isolated, one obtain the flux density as $\mathbf{B} = -\mu_0\nabla\Theta$. **Figure 4** shows the magnetic potential on the surface of the rotor together with some flux density lines.

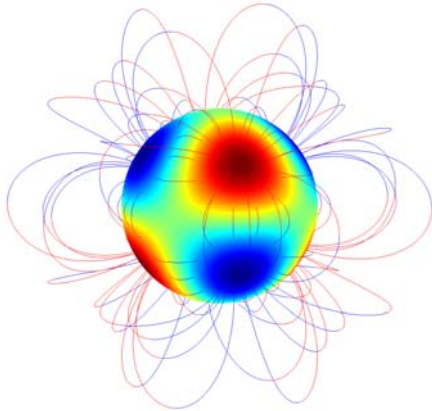


Figure 4: potential and flux lines

The force $\tilde{\mathbf{F}}$ exerted by a coil can be computed as indicated in [1]:

$$\tilde{\mathbf{F}} = \int_V \mathbf{J} \times \mathbf{B} dV \quad (2)$$

which integrates over the volume V of the coil the cross product of the current density \mathbf{J} with the flux density \mathbf{B} of the rotor. Since the force depends on the orientation of the rotor, the latter can be described by a rotation matrix $\tilde{\mathbf{R}}$ combining a rotation α about z , followed by a rotation β about x . This transformation allows any point of the rotor to be brought under the coil.

Subsequently, by defining the coordinate transformation $(x' \ y' \ z')^T = \tilde{\mathbf{R}}^T (\sin\theta \cos\phi \ \sin\theta \sin\phi \ \cos\theta)^T$, one can obtain the expression for the force:

$$\tilde{\mathbf{F}} = \frac{-\sqrt{3}\pi B_0 r_2^3 J}{32} \sin\theta (\cos^2\theta - 1) \left(21 \cos^2\theta - 1 \right) \cdot \left[\left(\frac{r_2}{R_a} \right)^2 - \left(\frac{r_2}{R_b} \right)^2 \right] \cdot \begin{pmatrix} \sin\beta \cos\beta (2 \cos^2\alpha - 1) \\ \sin\beta \sin\alpha \cos\alpha (3 \cos^2\beta - 1) \\ 4 \cos\beta \sin\alpha \cos\alpha (\cos^2\beta - 1) \end{pmatrix} \quad (3)$$

Note that, in order to simplify the notation, the form in Equation (3) expressed the indefinite integral for θ . The correct expression is $\tilde{\mathbf{F}} \Big|_{\theta_b}^{\theta_a} - \tilde{\mathbf{F}} \Big|_{\theta_a}^{\theta_b}$. In Equation (3), R_a and

R_b define the internal and the external radius of the coils while θ_b and θ_a the angles that describe their circular surface. Similarly, the torque $\tilde{\mathbf{T}}$ is obtained by taking the cross product of the application points of the infinitesimal forces by their value:

$$\tilde{\mathbf{T}} = \int_{R_a}^{R_b} \int_{\theta_a}^{\theta_b} \int_{\pi}^{\pi} \begin{pmatrix} r \sin\theta \cos\phi \\ r \sin\theta \sin\phi \\ r \cos\theta \end{pmatrix} \times (\mathbf{J} \times \mathbf{B}) r^2 \sin\theta \, d\phi \, d\theta \, dr \quad (4)$$

Finally,

$$\tilde{\mathbf{T}} = \frac{3\sqrt{3}\pi B_0 r_2^4 J}{32} \left[\frac{r_2}{R_a} - \frac{r_2}{R_b} \right] \begin{pmatrix} 10 \cos^3\theta \sin\theta - 9 \cos\theta \sin\theta - \theta \\ \sin\alpha \cos\alpha (3 \cos^2\beta - 1) \\ -\cos\beta (2 \cos^2\alpha - 1) \\ 0 \end{pmatrix} \quad (5)$$

Similar developments have been performed for a shielded stator. A shielded stator improves the efficiency of the system by a factor approximately 4. In addition, the shield prevents the magnetic field to disturb sensitive instruments that may be located in the neighborhood of the Reaction Sphere. On the other hand, however, the magnetic field of the spinning rotor induces important eddy currents in the iron shield that may impose constraints on the maximum rotating speed. For this reason, materials other than iron will be investigated so as to have good ferromagnetic quality but low electrical conductivity.

3.2. Electromechanical model

Dynamics

Newton's equations apply to describe the reaction sphere dynamics:

$$m_0 \frac{d}{dt} [S\mathbf{v} + \mathbf{v}_0] = S\mathbf{F} \quad (6)$$

$$\frac{d}{dt} [S\mathbf{A}] = S\mathbf{v} \quad (7)$$

where \mathbf{v} represents the translational velocity vector (stator frame), \mathbf{v}_0 the velocity of the stator origin 0 expressed in the inertia reference frame, S the stator frame in the inertia referential frame, and m_0 the rotor mass. Similarly, we can write the rotational speed equations:

$$J \frac{d}{dt} [S\boldsymbol{\omega}] = S\mathbf{T} \quad (8)$$

$$\frac{d}{dt} [SR] = S\boldsymbol{\omega} \times SR \quad (9)$$

with $\boldsymbol{\omega}$ the rotational speed vector and R the rotation matrix describing the rotor frame.

Force and Torque

Assuming that the rotor rotated to an orientation described by the rotation matrix R , one can, for each coil about a pole \mathbf{P}_i , identify the α_i and β_i values. The force $\tilde{\mathbf{F}}_i$ and torque $\tilde{\mathbf{T}}_i$ for each coil in a reference frame such that the z-axis is the axis of the coil can be computed by equations (3) and (5). Summing these forces and torques in a common reference frame allow to express them such that a matrix multiplies the current vector \mathbf{i} :

$$\begin{aligned} \mathbf{F} &= K_F(R) \cdot \mathbf{i} \\ \mathbf{T} &= K_T(R) \cdot \mathbf{i} \end{aligned} \quad (10)$$

The matrices K_F and K_T , which depend on the rotor orientation, can be estimated by first measuring the flux density through flux sensors.

3.3. System simulation

The mathematical model described in the previous section has been implemented in a Matlab/Simulink model. The model outputs are the three components of the torque vectors \mathbf{T} and \mathbf{F} while the inputs are the twenty components of the coil current \mathbf{i} . The states of the system are:

- the position of the rotor, i.e., the vector SA, 3 components

- the orientation of the rotor, i.e., matrix SR, 9 components
- the velocity of the rotor, i.e., vector Sv+v0, 3 components
- the angular velocity of the rotor, i.e., vector Sω, 3 components
- the current in the coils, i.e., vector i, 20 components

This Simulink model has been used for the development of a control algorithm.

4. ELECTROMAGNETIC DESIGN

In order to obtain a valid approximation of the theoretical flux distribution, we apply around the reaction Sphere surface a mosaic of small magnets (1.4 T) having different heights, as shown in **Figure 5**. Some resin may fill in the gaps to get a perfectly round sphere (needed for the position measurement).

The field generated by the magnets in the solid sphere quarters is high enough to fully reach saturation. This is important, because in this case, the permeability seen by an external field is close to the vacuum permeability. As a consequence the external field entering the rotor remains weak and so do the eddy currents. Therefore, solid motor steel can be used, which is both beneficial for the manufacture and for the symmetry (sheet steel would break the symmetry). The rotor is hollow to optimize the inertia-moment-to-mass ratio.

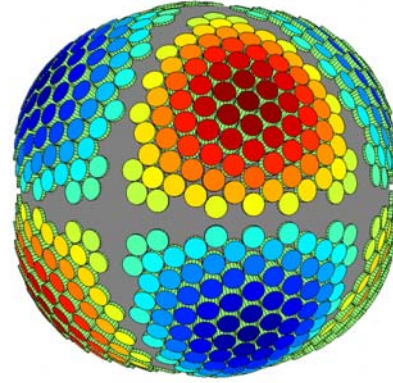


Figure 5: Rotor realization

In order to employ the selected optical position sensors, the rotor has been covered with a spherical layer made of Acrylonitrile Butadiene Styrene (ABS), as shown in **Figure 6**.



Figure 6: Rotor with its cover

5. REACTION SPHERE INSTRUMENTATION

In order to determine the Reaction Sphere position inside the stator, three position sensors are used. The latter require a smooth and white rotor surface. Furthermore, as discussed in the next section, the rotor orientation is determined using nine arrays of four CY-P3A flux sensors properly adjusted around the internal stator surface. To measure the exported torque, three Kistler torque sensors will be used.

6. ORIENTATION ESTIMATION

6.1. Problem Formulation

The orientation of the rotor defines force and torque characteristics through matrices K_F and K_T as in Equation (10). The rotor and stator references frames are related through the rotation matrix R that defines the orientation of the rotor. In the current framework, the rotation matrix R is described using Euler's parameters q_1, q_2, q_3 and q_4 . Therefore, parameters q_1, q_2, q_3 and q_4 have to be computed to determine the orientation of the rotor. Finally, observe that because of the pole symmetry in the rotor, similar force and torque characteristics can be obtained with different orientations.

6.2. Measuring Description

The radial flux density at the internal stator is given by

$$B_n = \frac{(x \ y \ z)}{R_1} \mathbf{B} = a \cdot xyz \quad (11)$$

where \mathbf{B} is the flux density outside the rotor and a is a scaling factor. The flux density S_j measured with a flux sensor at the position \mathbf{P}_j satisfies the relation

$$\prod_{i=1}^3 (R^T \mathbf{P}_j)_i = S_j \quad (12)$$

where R is the rotation matrix defining the rotation of the sphere with respect to the stator. The number of necessary sensors to uniquely determine an equivalent orientation is unknown and not trivial to investigate. Numerical simulations allowed us to fix the minimum

number of flux sensors to 8. These flux sensor are properly adjusted around the inner surface of the stator.

6.3. Orientation Computation

The orientation R of the sphere is computed given eight magnetic flux measurements S_1, S_2, \dots, S_8 , at locations $\mathbf{P}_1, \mathbf{P}_2, \dots, \mathbf{P}_8$ satisfying

$$\mathbf{r}(\mathbf{q}) = \begin{pmatrix} \prod (R^T \mathbf{P}_1)_i - S_1 \\ \prod (R^T \mathbf{P}_2)_i - S_2 \\ \vdots \\ \prod (R^T \mathbf{P}_8)_i - S_8 \\ w(q_1^2 + q_2^2 + q_3^2 + q_4^2 - 1) \end{pmatrix} = 0 \quad (13)$$

where w is a weighting scalar. A unique solution can be found solving the system of equations numerically for instance with a line search Newton method or more sophisticated algorithm such as trust-region methods.

7. CONTROL ALGORITHM DESIGN

As depicted in **Figure 7**, two dynamic controllers have been developed to control the reaction sphere position and the exported torque. The dynamic controllers output force and torque vectors that are subsequently translated into currents by a minimal energy inverse model thanks to matrices K_F and K_T . The system linearity allows summing the current contributions for the bearing and for the torque. For the reaction sphere position, the controller is made of a cascade of position and speed controllers. The speed is derived from the measured position with appropriate filtering. The torque controller was replaced by a controller of the rotational speed which will be more convenient to operate on a real breadboard system. This controller imposes a speed of rotation vector in 3 axis to the rotor. Both dynamic controllers rely on monovariable state-space design, with feed-forward and integral components. They include limitations of the commanded torque and force outputs. When the limitations are reached, the integrator of the controller is corrected to avoid control overshoot at de-saturation..

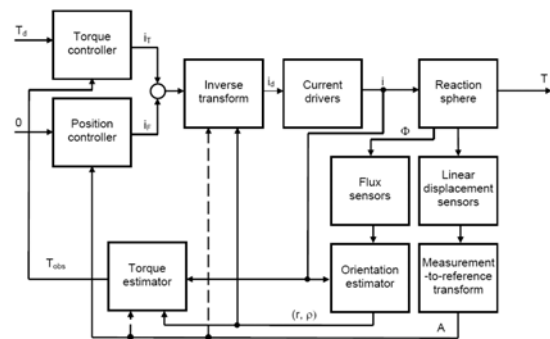


Figure 7: Position and torque control diagram

8. COMMAND ELECTRONIC

The developed dedicated electronic rack is displayed in *Figure 8*.



Figure 8: Command electronic

This command electronic includes 20 linear current amplifiers that rely on the CSEM Intelligent Motion Control Unit. It receives its current references from a dSpace DS1105 external platform, on which the control algorithms are to run for test purposes. The experimental setup is presented in *Figure 9*.

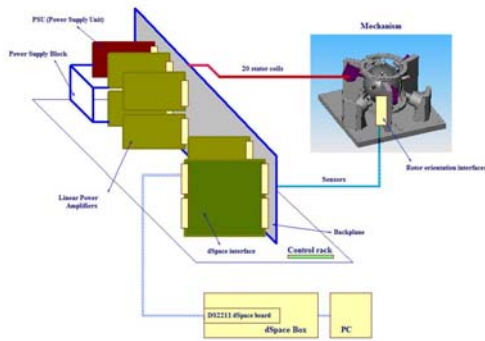


Figure 9: General configuration

9. REACTION SPHERE INTEGRATION

The Reaction Sphere requires a careful integration process. The twenty coils are adjusted inside the stator. Then, the magnets are attached to the rotor surface using developed techniques to avoid them to stuck together. Finally, the rotor is adjusted inside a stator half and the two halves subsequently integrated. *Figure 10* shows the stator and rotor before their integration.



Figure 10: Stator and rotor integration

10. PRELIMINARY TEST RESULTS

In order to validate the Reaction Sphere model as well as its performances, some preliminary tests have been performed and several others are scheduled. The following parameters have been so far measured:

- the magnetic flux and position sensor offsets
- current amplifiers offsets and gains
- coils resistances

Preliminary rotation tests have also been performed. Based on a determined rotor orientation, a current distribution has been calculated so as to obtain a desired rotation.

11. CONCLUSIONS

A Reaction Sphere prototype has been manufactured based on a synchronous motor concept. The rotor is an eight pole permanent magnet rotor, with a hollow iron core, whereas the stator has 20 poles.

We have developed an analytical model of the Reaction Sphere that has led to a Matlab/Simulink model, which has been used as designing platform for the controller synthesis and simulation.

A dedicated command electronic comprising 20 linear current amplifiers has also been developed to drive the Reaction Sphere.

Preliminary tests to validate the Reaction Sphere model as well as its performances have been performed and several others are scheduled.

12. REFERENCES

- [1] Fred Gardiol, *Traité d'Electricité, volume III, Electromagnétisme*, Presses Polytechniques Romandes.